Ukrainian Journal of Physical Optics
ISSUE 4
2025

HEAT TREATMENT EFFECT ON OPTICAL ABSORPTION AND PHOTOLUMINESCENCE IN $Na_{0.5}Bi_{0.5}TiO_3$ CRYSTALS

T. V. PANCHENKO[1*], V. M. SIDAK[1], M. P. TRUBITSYN[1,2], V. LAGUTA[2,3], O. V. KHMELENKO[1], T. V. KRUZINA[1]

[1]Research Institute for Energy Efficient Technologies and Materials Sciences,
Oles Honchar Dnipro National University, Science Avenue 72, Dnipro, 49010, Ukraine
[2]Institute of Physics of the Czech Academy of Sciences, Na Slovance 1999/2, 182 00 Prague 8, Czech Republic
[3]Frantsevich Institute for Problems of Materials Science, NAS Ukraine, Omelyan Pritsak str. 3, Kyiv, 03142, Ukraine
*Corresponding author: panchtv141@gmail.com

Received: 23.05.2025

Abstract. Optical absorption and photoluminescence spectra of as-grown and heat-treated sodium-bismuth titanate $Na_{0.5}Bi_{0.5}TiO_3$ single crystals are studied. The heat treatment was performed in air and vacuum at $T_{ann} = 1070$ K. Optical absorption and photoluminescence were measured in the spectral range of 1.5 to 3.3 eV. It is found that treatment in air decreases optical absorption, while subsequent treatment in vacuum increases it. Excitation of the as-grown crystal near the edge of the fundamental optical absorption (~2.95 eV) induces intense violet (~2.83 eV) and weak green (~2.25 eV) photoluminescence. Both heat treatment in air and vacuum reduce the intensity of the violet and green photoluminescence bands. The effects of heat treatment on optical absorption and photoluminescence are attributed to electronic transitions in Ti^{3+} centers, which compensate for the excess charge of oxygen vacancies and are located within trigonally and tetragonally distorted oxygen octahedra.

Keywords: optical absorption, photoluminescence, heat treatment, oxygen vacancy, $Na_{0.5}Bi_{0.5}TiO_3$ crystal
UDC: 535.3, 548.4
DOI: 10.3116/16091833/Ukr.J.Phys.Opt.2025.04001

1. Introduction

The phenomena of optical absorption and luminescence in solids form the basis for the operation of sensors, liquid crystal displays, light-emitting diode displays, lighting systems, optical thermometers, and more [1-3]. Today, many oxides, sulfides, sulfates, vanadates, phosphates, and aluminates exhibit promising optical absorption and luminophore properties. The Ti-containing complex oxides with a perovskite structure are particularly interesting because they integrate optical absorption and luminescence with effects from physical optics [3-5]. The instability of the crystal lattice during structural phase transitions is crucial for designing functional materials for optoelectronics and nonlinear optics.

Polar properties and high susceptibility to external factors contribute to the widespread use of perovskites and related compounds in devices for generating, detecting, converting electric signals, and storing information. Introducing different ions with the same or different valences into A- or B-type sites in the perovskite structure ABO_3 has proven to be an effective method for obtaining highly efficient functional materials. Sodium-bismuth titanate $Na_{0.5}Bi_{0.5}TiO_3$ (NBT) crystal serves as an example of this approach, where monovalent Na^+ ions and trivalent Bi^{3+} ions occupy the A-type positions [6-8]. It is remarkable that, according to the available data, there is no chemical ordering of sodium and bismuth ions in the A-type sites of the NBT lattice [7,8]. *Ab initio* calculations [9] showed that the different valencies of Na^+ and Bi^{3+} ions occupied the same A-type site, leading to this chemical disorder. The NBT crystal exhibits high dielectric permittivity and piezoelectric coefficients. The forbidden zone width ~3 eV [10] causes transparency of NBT crystals in the visible wavelength range of the optical spectrum. Due to their lead-free chemical composition, solid solutions of NBT-$BaTiO_3$ are now regarded as the most promising eco-friendly materials available to replace lead-based piezoelectrics in electromechanical converters and transducers [7,8].

On cooling NBT crystal undergoes the following sequence of phase transitions [11]: in the range ~813 – 773 K from the paraelectric cubic phase (symmetry space group Pm3m) to the non-polar tetragonal phase (space group P4/mbm refined in [12,13]), and on further cooling at ~673–528 to the ferroelectric rhombohedral phase (group R3c). In the range 673–528 K, the rhombohedral and tetragonal phases coexist and dielectric permittivity $\varepsilon(T)$ exhibits broad maximum at T_m~593 K [14]. The specific frequency dispersion of ε, observed around T_m is typical for ferroelectric relaxors [7,8] and is associated with reorientations of rhombohedral polar nanoregions immersed in a non-polar tetragonal matrix.

For materials used in practice, it is important to have complete information about typical crystal lattice defects, their influence on valuable properties, and to develop technologies for controlling the content of such defects. Moreover, in crystals exhibiting structural phase transitions, the role of defects becomes particularly significant [15]. Numerous studies investigate the lattice defects in titanium-containing complex oxides with a perovskite structure. However, information about the NBT crystal is extremely scarce. Considering the different ion valences and the intrinsic disorder in the Na^+/Bi^{3+} sublattice, one can assume that structural defects significantly influence the physical properties of the NBT crystal.

Earlier low-frequency dielectric relaxation observed in NBT [16] was attributed to associated dipole complexes, which were thermally decomposed upon heating. Heat treatment of NBT crystals in air and in vacuum strongly influenced the dielectric anomaly and evidenced that oxygen vacancies (V_O) played a key role in the observed dielectric relaxation and marked role in charge transfer processes [17,18]. Additionally, heat treating significantly altered the optical transparency of the NBT crystals. Thus, heat treatment affects the content of the defects, which demonstrate both electrical and optical activity.

Up to now, mainly structural, ferroelectric, and electrophysical properties of NBT crystal and ceramics have been investigated in detail [8,11]. Optical absorption has been studied insufficiently [10], whereas luminescence has not been considered at all. In the present work, we study optical absorption and photoluminescence in as-grown and heat-treated NBT crystals. The purpose of this paper is to clarify the nature of the defects that influence the optical properties of the NBT crystal.

2.Experiment

NBT single crystals were grown by the Czochralski method in an ambient atmosphere. The as-grown crystals were homogeneous and optically transparent (Fig. 1, a). The samples were prepared as the polished plates, with their principal planes aligned with the crystallographic plane (111). The thickness of the samples was d = 0.2 mm. The optical properties were measured on untreated samples, which were cut from the as-grown single-crystalline NBT boule, as well as on samples that were heat-treated in air at T_{ann} = 1070 K for 1 h and then in vacuum at the same temperature, T_{ann}, for 2 h. After each treatment, the samples were slowly cooled to room temperature. Fig. 1 displays the as-grown NBT single crystal, the untreated sample, and the samples that were heat-treated in air and in vacuum. Heat treatment in air slightly improved the optical transparency of the samples, while annealing in vacuum led to a noticeable darkening of the samples.

The stationary optical transmittance spectra for the untreated $t_0(\nu)$, annealed in air $t^{air}(\nu)$ and in vacuum $t^{vac}(\nu)$ samples were recorded by using spectrophotometer Specord M40 at the temperature 80 K in the wavelength range λ=370-900 nm (energy of light quanta $h\nu$=3.3-1.38 eV, where $\nu=10^3/\lambda$ cm^{-1}). The corresponding optical absorption spectra $\alpha_0(h\nu)$, $\alpha^{\mathrm{air}}(h\nu)$ and $\alpha^{\mathrm{vac}}(h\nu)$ were calculated from the transmittance $t(h\nu)$ by using the known relation:

$$t(h\nu) = {((1-R)^2 \cdot \exp(-\alpha d))} \Big/ {\left(1-R^2 \exp(-2\alpha d)\right)} . \tag{1}$$

The reflection spectrum $R(h\nu)=(1-n)/(1+n)$ in Eq. (1) was determined from the refractive spectrum $n(h\nu)$ reported in [19].

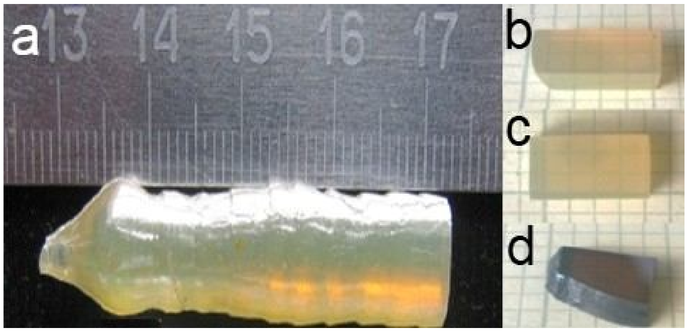

Fig. 1. NBT crystal grown by the Czochralski method (a), the untreated sample (b), and the samples after heat treating in air (c) and in vacuum (d).

The photoluminescence excitation spectra $I^{PLE}(h\nu)$ and photoluminescence emission spectra $I^{PL}(h\nu)$ were measured at room temperature (~295 K) in the same optical range as the absorption spectra. The excitation of photoluminescence was performed by a xenon lamp DKsL-1000 with the help of an MDR-2 monochromator. The $I^{PLE}(h\nu)$ and $I^{PL}(h\nu)$ spectra were registered by the MDR-12 monochromator with the help of a cooled to 250 K photomultiplier tube FEU-136 operating in the photon counting mode.

3. Results and discussion

3.1. Optical absorption

Fig. 2a shows the stationary optical absorption spectra for the as-grown and heat-treated NBT crystals. In the interval $h\nu$=1.5-3.0 eV, the optical absorption $\alpha_0(h\nu)$ of the untreated sample reaches the value α_0~30 cm^{-1} and changes slightly with the energy of light quanta (curve 1 in Fig. 2 a). The value α_0=300 cm^{-1}, obtained at $h\nu$=3.2 eV, gives an estimation of the band gap width $\Delta E_g \approx 3.2$ eV, which is somewhat higher than the value $\Delta E_g \approx 3.0$ eV reported in [10]. In the region of the fundamental absorption edge, i.e., at $h\nu > 3.0$ eV, $\alpha_0(h\nu)$ shows the nearly exponential growth. Such behavior indicates that in this interval, optical absorption is determined by the transitions from the local energy states adjacent to the ceiling of the valence zone or to the bottom of the conduction zone. The character of the dependence $\alpha_0(h\nu)$ reflects the exponential distribution of the local states density within the forbidden zone, with the formation of a so-called 'tail' of states.

After heat treating in air, the absorption of NBT crystal decreases in the spectral range $h\nu = 1.5$-3.0 eV, while in the edge absorption interval $h\nu > 3.0$ eV, $\alpha^{air}(h\nu)$ changes insignificantly (curve 2 in Fig. 2a). Subsequent annealing in vacuum increases the optical absorption $\alpha^{vac}(h\nu)$ (curve 3 in Fig. 2a).

To characterize the effects of the heat treatment, the differences of the absorption spectra $\Delta\alpha_1(h\nu) = \alpha^{air}(h\nu) - \alpha_0(h\nu)$ and $\Delta\alpha_2(h\nu) = \alpha^{vac}(h\nu) - \alpha^{air}(h\nu)$ are plotted in Fig. 2b. The difference absorption $\Delta\alpha_1(h\nu)$ is negative, it passes through a blurred minimum at ~2.0 eV and shows less structured anomalies in the range 2.3-3.0 eV. The dependence $\Delta\alpha_2(h\nu)$ in the studied range is positive. It exhibits weakly distinguishable maximums in the interval 2.0-2.8 eV, shows a more distinct peak at $h\nu = 2.95$ eV, and decreases sharply at $h\nu > 3.1$ eV. The dependences $\Delta\alpha_{1,2}$ are weakly structured (Fig. 2b). Nevertheless, the treatment effects are unambiguous: treating in air decreases absorption (negative $\Delta\alpha_1$), whereas treating in vacuum increases absorption (positive $\Delta\alpha_2$).

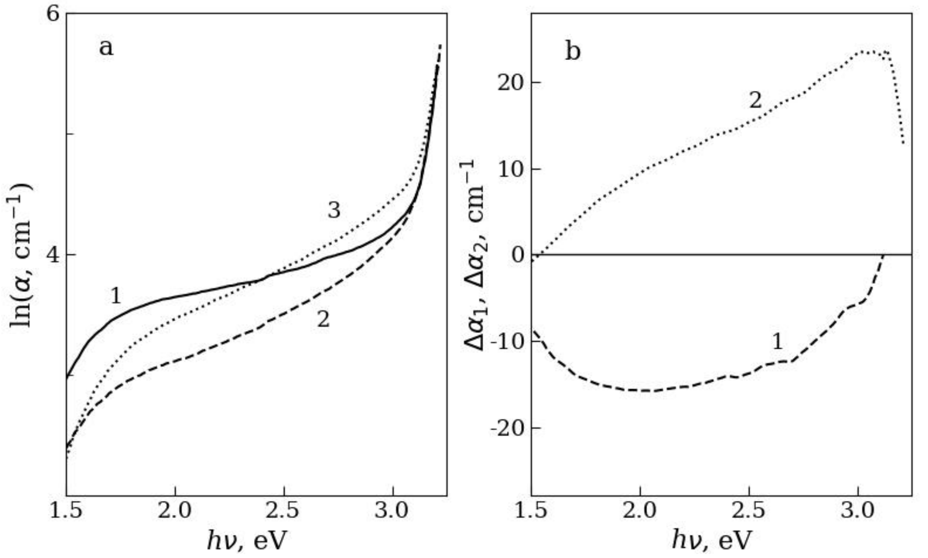

Fig. 2. (a) Absorption spectra of the untreated NBT crystal $\alpha_0(h\nu)$ (curve 1), and of the crystals treated in air $\alpha^{air}(h\nu)$ (curve 2) and treated in vacuum $\alpha^{vac}(h\nu)$ (curve 3). All the spectra were measured at $T = 80$ K. (b) The differences of the optical absorption $\Delta\alpha_1$ (curve 1) and $\Delta\alpha_2$ (curve 2).

According to [20], in the range of $T_{ann} = 1070$ K in the NBT crystal lattice, the oxygen sublattice softens only while the cation sublattices remain quite rigid. It means that at T_{ann}, oxygen ions become mobile enough and the crystal lattice can exchange oxygen with the surrounding atmosphere. Thus, treating in air should decrease the concentration of oxygen vacancies V_O. On the other hand, treating in a vacuum should increase the concentration of

V_O. Let's consider the nature of the defects that change the absorption spectrum after thermal treatments (Fig. 2).

Oxygen vacancies are the typical defects in oxide crystals. Nevertheless, V_O themselves are optically inactive and does not affect absorption spectra. The appearance of an oxygen vacancy locally introduces a charge imbalance (excess positive charge (+2)) into the lattice and requires the emergence of additional defects with a negative effective charge (-2). Therefore, one can anticipate that the treatment's effects on the optical absorption (Fig. 2) can be attributed to the defects that compensate for the excess charge of V_O and exhibit optical activity. Often, the electroneutrality of the crystal lattice with V_O can be attributed to charge-compensating electron centers, in which an electron is wholly or partly localized on the orbitals of neighboring cations, such as Ti. Oxygen vacancies can also stimulate the creation of free electrons in the conduction band. These electrons can also be self-trapped at Ti ions via a polaronic mechanism, similar to that in $BaTiO_3$ [21,22].

In the tetravalent state the titanium ion (Ti^{4+}) has an electronic configuration of $3d^0$ and is optically inactive. By trapping an electron trivalent titanium Ti^{3+} has an electronic configuration of $3d^1$ and becomes optically active. The ground state of the free Ti^{3+} ion corresponds to the fivefold degenerated term ^2D. The scheme of ^2D term splitting in the ligand's crystal field is shown in Fig. 3. In the crystal field of octahedral symmetry, the ^2D term splits into a threefold degenerated term $^2T_{2g}$ and a twofold degenerated term ^2E_g.

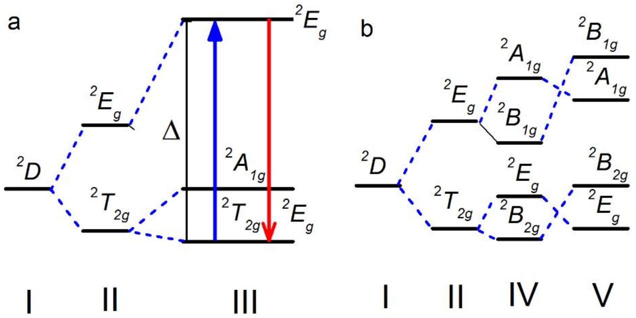

Fig. 3. (a) ^2D term of free one-electron ion (I) and its splitting in the octahedral crystal field (II), trigonally distorted octahedron (III), and (b) tetragonally compressed (IV) or stretched (V) octahedron. The transitions corresponding to luminescence excitation and emission are shown by arrows in diagram (III).

Crystal field theory shows that the state of one-electron transition metal ions in an octahedral crystal field is not in equilibrium. Stabilization of such ion states occurs through distortion of the octahedral complexes due to the Jahn-Teller effect [4, 23-25]. The distortion of the octahedra can occur alternatively along the trigonal <111> axis or along the tetragonal <100> axis depending on the ratio between the parameters of electron-phonon interaction [25]. Therefore, when interpreting optical spectra, it is necessary to take into account that the appearance of Ti^{3+} centers should be accompanied by trigonal or tetragonal distortion of oxygen octahedra. Besides, it should be remembered that the absorption spectra were measured in the ferroelectric phase (T=80 K) where the crystal lattice of NBT was already trigonally distorted. Thus, trigonal perturbation can be considered as the main type of the $(Ti^{3+})O_6$ octahedra distortion in NBT crystal.

In the trigonally distorted octahedral, the titanium ground state level $^2T_{2g}$ splits into two sublevels, ^2E_g, which energetically coincide with $^2T_{2g}$ and $^2A_{1g}$ [4,23] (Fig. 3a, III). The transitions $^2T_{2g}$ (^2E_g) → ^2E_g give rise to the absorption band observed in the interval Δ = (2.5-3.1) eV for a number of minerals [4,23] (Fig. 3a, III). The spectral position of this band makes it possible to determine the crystal field strength $Dq = 0.1\Delta$ (Fig. 3a, III).

As discussed above, the intense absorption band at $h\nu_{max} = \Delta = 2.95$ eV (23790 cm^{-1}) dominates in the spectrum $\Delta\alpha_2(h\nu)$ and is less clearly visible in the spectrum $\Delta\alpha_1(h\nu)$ (Fig. 2, b). The spectral position indicates that this band can be associated with electronic transitions $^2T_{2g}(^2E_g) \rightarrow {}^2E_g$ in Ti^{3+} ions within trigonally distorted oxygen octahedra (Fig. 3a, III). In this case, the crystalline field strength is Dq = 2379 cm^{-1} (Fig. 3a, III). Nevertheless, this mechanism cannot explain the effects of heat treatments on optical absorption at lower energies ($h\nu$~1.8-2.8 eV), where $\Delta\alpha_1$ shows a broad minimum at ~ 2.0 eV, whereas $\Delta\alpha_2$ demonstrates a few broad and weakly structured maxima.

The optical absorption in this range $h\nu$~1.8-2.8 eV can be associated with electronic transitions in Ti^{3+} ions within tetragonally distorted oxygen octahedra (Fig. 3, b, IV, V). This type of distortion can appear when V_O and charge-compensating Ti^{3+} centers form associated pairs [22,26]. In such a paired complex, the oxygen octahedron turns out to be distorted along the Ti^{3+}-V_O bond, i.e., it undergoes strong tetragonal distortion, while the trigonal distortion due to the Jahn-Teller effect or ferroelectric state plays a minor role. The "pure" tetragonal distortion splits the T_{2g}, E_g terms into the four sublevels (Fig. 3b).

The optical absorption caused by these centers (Fig. 3b) is characterized by the transitions $^2B_{2g} \rightarrow {}^2E_g$, $^2B_{2g} \rightarrow {}^2B_{1g}$, $^2B_{2g} \rightarrow {}^2A_{1g}$ (Fig. 3b, IV, V). These transitions give rise to the three absorption bands observed in the Ti-containing crystals at $h\nu_{max}$~1.6 eV (13000 cm^{-1}), 2.2 eV (18000 cm^{-1}), and 4.1 eV (33000 cm^{-1}), respectively [27]. The two low-energy bands from the latter correspond to the interval ~1.8-2.8 eV, where $\Delta\alpha_1$ shows a diffuse minimum (~2.0 eV) and $\Delta\alpha_2$ has weakly structured maximums (Fig. 2b).

One should add that the optical absorption bands in the whole studied range are sufficiently broadened. Broadening of the 2.95 eV band evidences for charge transfer from the Ti^{3+} center to the nearest titanium Ti^{4+} ion through the orbitals of the intermediate oxygen, which binds these two ions. This corresponds to the presence of small-radius polarons. Moreover, one should account for the true symmetry of the Ti^{3+}-V_O centers, which is reduced to a monoclinic group due to the combination of a weaker trigonal distortion and a stronger tetragonal one. This symmetry-lowering induces additional electronic transitions, which remain unresolved and cause smearing of the absorption envelope contour in the 1.8-2.8 eV interval.

The proposed models of the defects that influence the optical absorption of the NBT crystal are schematically illustrated in Fig. 4.

It should also be noted that the trigonal and tetragonal distortions of oxygen octahedra may have another nature, which is not directly related to defects or phase state, but results from the intrinsic structural disorder in the NBT crystal lattice. As mentioned above, in the NBT lattice, the positions of Na^+ and Bi^{3+} ions are chemically disordered in the A-type sites of the ABO_3 structure. At the same time, consideration of only ionic bonds allows one to expect Na^+/Bi^{3+} chemical ordering. The results of *ab-initio* calculations performed in [9] cleared up the reasons for this disorder. The authors of [9] analyzed the thermodynamic stability of different configurations of Na^+/Bi^{3+} distributions in the A-type sites. It was supposed that oxygen ions

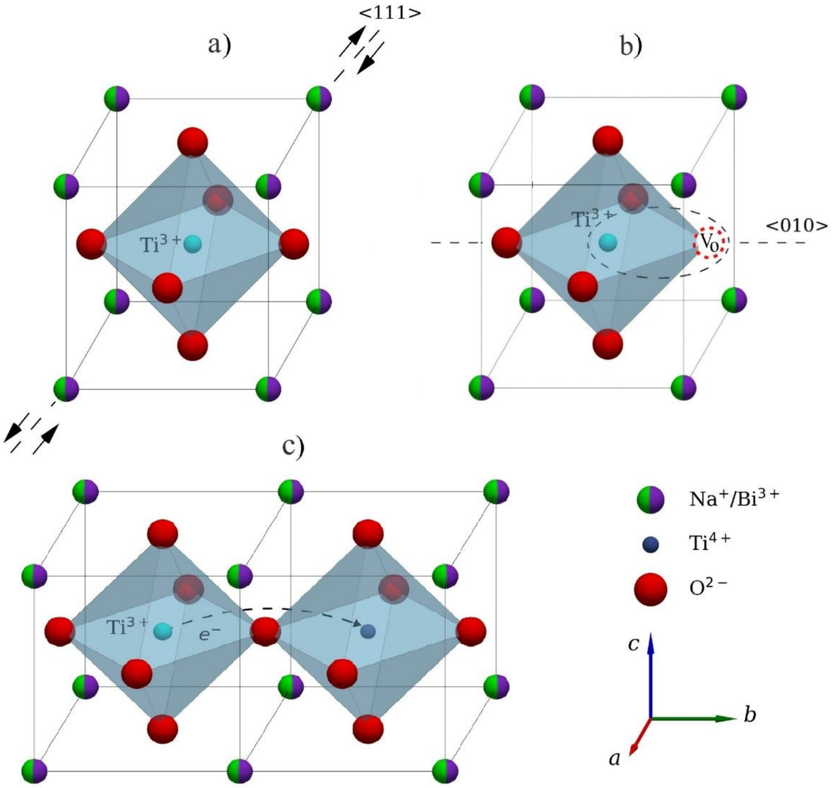

Fig. 4. Fragment of NBT crystal structure with Ti^{3+} center within a trigonally distorted oxygen octahedron (a), Ti^{3+}-V_O pair center resulting in strong tetragonal distortion of the oxygen octahedron (b), electron transfer through regular titanium ions (Ti^{3+} small radius polarons) (c).

could shift from the ideal lattice site to stabilise certain configurations of neighbouring Na^+/Bi^{3+} ions and to relax the local structure [9]. The calculations showed that the local lattice relaxation made more stable exactly those Na^+/Bi^{3+} configurations which were most unstable for the ideal non-relaxed perovskite structure with pure ionic interaction. Besides, the energy difference between the most stable relaxed Na^+/Bi^{3+} configurations was found to be twice as small as the entropy contribution from the configurations mixing to the free energy. The critical temperature, above which the chemical ordering is found to be unfavorable, was estimated as ~570 K, which was much lower than the temperature of NBT crystal growth (~1570 K) [28]. Thus, a few Na^+/Bi^{3+} relaxed configurations can appear with close probability, and corresponding chemical ordering can exist only on a short-range scale. It is noteworthy that the most probable relaxed configurations, found in [9], correspond just to the trigonal and tetragonal distortions of the original structure.

The results reported in [9] point out the important difference between the structures of classical perovskites with ABO_3 structure, where A-type sites are occupied by ions of the same chemical element, and the perovskites with $A'A''BO_3$ structure, where the same sites are occupied by A' and A'' ions with different valences. In the lattice of the formers ($BaTiO_3$, $CaTiO_3$, $SrTiO_3$, and others), undistorted oxygen octahedra can exist in the absence of any defects. In the NBT crystal, the oxygen octahedra are trigonally and tetragonally distorted because the A-type sites are occupied by differently charged Na^+/Bi^{3+} ions. Hence, considering the absorption spectra of NBT (Fig. 2), there is no need to involve additional arguments on the Jahn-Teller effect and the emergence of associated Ti^{3+}-V_O pairs to interpret trigonal and tetragonal distortions of the oxygen octahedra with trivalent titanium ions. The presence of the trigonally and tetragonally distorted octahedra can be considered as an intrinsic feature of the NBT crystal lattice, peculiar to all structural phases. One can hope that a detailed study of the optical absorption edge and the magnetic resonance (EPR, NMR) spectra could help to clear up the physical reasons for oxygen octahedra distortions in the NBT lattice.

It is of interest to follow the correlation of the heat treatment effects on optical absorption (Fig. 2) with low-frequency dielectric relaxation found in the NBT crystal earlier [16-18]. Similarly to the data shown in Fig. 2b, relaxation anomaly $\varepsilon(T)$ was observed in the as-grown NBT crystal and disappeared after being treated in air. Subsequent treatment in vacuum allowed to restore and even to enhance the $\varepsilon(T)$ anomaly. Accounting for the intensity of $\varepsilon(T)$ maximum ($\sim 10^4$) and its specific frequency dispersion [29], the observed dielectric relaxation was attributed to mobile electron defects accumulated near the boundaries of nanopolar rhombohedral regions distributed in a non-polar matrix with tetragonal structure [30]. These defects were associated with Ti^{3+} centers, which compensate for the excess charge introduced by oxygen vacancies. Thus, Ti^{3+} centers, accompanying the appearance of V_O, exhibit both optical (Fig. 2) and electrical [29,30] activity.

3.2. Photoluminescence spectra

Fig. 5 shows the photoluminescence excitation and emission spectra measured in as-grown and heat-treated NBT crystals. The photoluminescence excitation spectrum $I^{PLE}(h\nu)$ (the inset to Fig. 5) represents a broad structureless band with a maximum at $h\nu^{PLE}_{\max} = 2.87$ eV ($\nu_{\max} = 23145$ cm^{-1}). The position of the $I^{PLE}(h\nu)$ maximum correlates with the absorption difference $\Delta\alpha_2(h\nu)$, which has a maximum at $h\nu^{PLE}_{\max} = 2.95$ eV ($\nu_{\max} = 23790$ cm^{-1}, Fig. 2b).

The $I^{PL}(h\nu)$ photoluminescence spectra show two broad structureless bands with $h\nu^{PL}_{\max1} = 2.83$ eV (22822 cm^{-1}, violet luminescence) and $h\nu^{PL}_{\max2} = 2.25$ eV (18145 cm^{-1}, green luminescence). Small Stokes shift $\Delta_{St} = h\nu^{PLE}_{\max} - h\nu^{PL}_{max1} = 0.04$ eV (322 cm^{-1}, Fig. 5) characterizes the violet photoluminescence band.

The correlation of the photoluminescence emission spectra $I^{PL}(h\nu)$ and absorption spectra $\Delta\alpha_2(h\nu)$ indicates an intracenter nature of the electronic transitions in Ti^{3+} ions within trigonally distorted oxygen octahedra (Fig. 2b and the inset to Fig. 5). Similar absorption bands with $h\nu_{\max} = 2.4$-3.1 eV ($\nu_{\max} = 19355 - 25000$ cm^{-1}) were attributed to electronic transitions in Ti^{3+} ions in many titanium-containing perovskites [3,4,23]. The green luminescence band at $h\nu^{PL}_{\max2}$ indicates the presence of luminescence centers of another nature. We suppose that this band is determined by trivalent titanium ions associated with oxygen vacancies Ti^{3+}-V_O in tetragonally distorted octahedra (Fig. 5).

Heat treatment in air gave the expected result. The treatment reduces the concentration of V_O and, accordingly, decreases the concentration of Ti^{3+} centers and associated Ti^{3+}-V_O pairs. Correspondingly, the photoluminescence intensity $I^{PL}(h\nu)$ drops down (Fig. 5, curve 2), as well as optical absorption decreases (Fig. 2a, curve 2).

Heat treatment in vacuum decreases the luminescence intensity again, which is an unexpected effect. Treatment in vacuum increases the concentration of Ti^{3+} centers and associated Ti^{3+}-V_O pairs, which is confirmed by the positive difference absorption $\Delta\alpha_2$

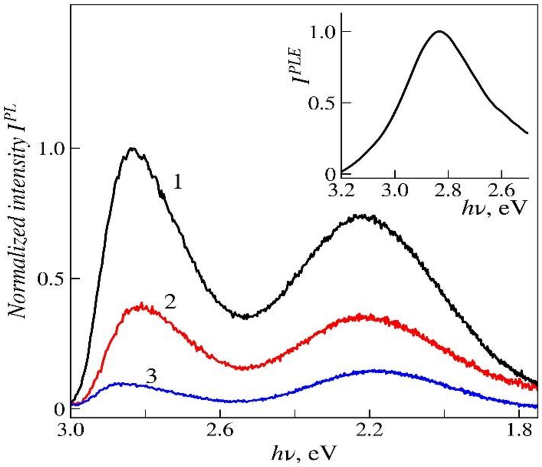

Fig. 5. The photoluminescence emission spectra $I^{PL}(h\nu)$ for the untreated NBT crystal (curve 1), the crystal heat-treated in air (curve 2), and the crystal heat-treated in vacuum (curve 3). The photoluminescence excitation spectrum $I^{PLE}(h\nu)$ is shown in the inset. The spectra were measured at T = 295 K.

(Fig. 2b). However, the photoluminescence intensity $I^{PL}(h\nu)$ decreases in this case (Fig. 5, curve 3). This behavior indicates that photoluminescence quenching processes start to play an essential role.

Intra-center quenching represents the possible mechanism when non-radiative electronic transitions occur in the luminescent Ti^{3+} centers ions and Ti^{3+}-V_O pairs (Fig. 4a, b). In this case, the absorbed energy of light quanta is spent on electron-phonon interaction, as well as on the relaxation of vibrations of the centers themselves. This mechanism is supported by the presence of the Stokes shift of the intra-center luminescence band Δ_{St}=0.04 eV (322 cm^{-1}).

Besides, external quenching is another possible mechanism, when non-radiative electronic transitions occur outside the luminescence centers. In this case, the absorbed energy is transferred through a large number of local levels in the forbidden zone. The presence of the Urbach's tail of the local levels density of states evidences in favor of this mechanism. These levels are responsible for the absorption growth near the edge of the forbidden zone after treating NBT crystals in a vacuum (Fig. 2, curve 3).

In both cases, the so-called concentration quenching of photoluminescence takes place, when the quenching intensifies with increasing concentration of luminescence and quenching centers. Apparently, that study of photoluminescence at low temperatures, investigations of the lattice vibrational spectra, as well as studies of defect structure by EPR and NMR, will help to propose more detailed models of photoluminescence centers and mechanisms of luminescence quenching in NBT crystals.

Considering the optical absorption and photoluminescence spectra of NBT crystals, the role of Bi^{3+} ions warrants additional comment. Blue and ultraviolet luminescence in perovskites doped with Bi^{3+} ions attracts close attention due to the prospects of applications in gamma radiation detectors, scintillators for X-ray imaging, and other devices [3]. In contrast to Bi^{3+}-doped perovskites, bismuth ions in NBT are the hosts forming the crystal and energy band structures.

Bi^{3+} ions have the electronic configuration $5d^{10}6s^2$, and optical transitions can occur between the ground singlet $^1S_0$ and the triplet levels $^3P_0$, $^3P_1$, as well as the singlet level $^1P_1$. In many perovskites, the luminescence spectrum corresponds to transitions the $^3P_{0,1}\rightarrow{}^1S_0$; at low temperatures the $^3P_0$ level emits, and at high temperatures, emission occurs from the $^3P_1$ state. A special mechanism of blue and ultraviolet photoluminescence occurs when the Bi^{3+} ion is located in a crystal lattice with nd^0 (n = 1, 2, ..., 5) cations. Provided that the level $^1S_0$ coincides with the ceiling of the valence zone, and the width of the forbidden zone is small, the excited levels of the Bi^{3+} ion fall into the conduction zone of the crystal, and the charge transfer of the 'metal-to-metal' type takes place. The luminescence is characterized by a large Stokes shift [3].

NBT crystals containing Ti^{4+} ions with the $3d^0$ electronic configuration have a conduction band width (~3.2 eV), so luminescence with charge transfer can be expected from Bi^{3+} ions. However, in perovskites doped with Bi^{3+} ions, such luminescence is excited at higher energies close to their forbidden zone widths: 3.65 eV ($CaTiO_3$:Bi [31]), 4.07 eV ($CaSnO_3$:Bi [32]), 4.27-5.39 eV ($LaInO_3$:Bi, $LaAlO_3$:Bi, $CaZrO_3$:Bi [33]). The luminescence is characterized by a large Stokes shift (Δ_{St}=2.1 eV [31], 2.74 eV [32], 0.75 – 1.12 eV [33]). In NBT crystals, luminescence excitation occurs at an energy of 2.85 eV, which is smaller than the forbidden band width. The Stokes shift (Δ_{St}= 0.04 eV) is also significantly smaller than in the mentioned perovskites. The above inconsistencies suggest that the role of Bi^{3+} ions in the excitation of violet photoluminescence in NBT crystals is insignificant. Confirmation of this assumption requires further research.

4.Conclusion

Optical absorption and photoluminescence spectra are studied in the range 1.5-3.3 eV in as-grown and heat-treated $Na_{0.5}Bi_{0.5}TiO_3$ crystals. It is shown that heat treatment in air decreases the optical absorption α, whereas treatment in vacuum increases α.

Excitation of $Na_{0.5}Bi_{0.5}TiO_3$ crystal at room temperature near the edge of the fundamental optical absorption (~2.95 eV) causes the appearance of broad bands of intense violet ($h\nu^{PL}_{max1}$=2.83 eV) and weak green ($h\nu^{PL}_{max2}$ = 2.25 eV) photoluminescence. Heat treatment in air as well as treatment in vacuum reduces the intensity of both violet and green photoluminescence.

The observed effects of heat treatments on optical absorption and photoluminescence spectra of NBT crystals are attributed to electronic transitions in Ti^{3+} centers located within distorted oxygen octahedra. The most intense optical absorption and photoluminescence bands are associated with the electronic transitions $^2T_{2g}(^2E_g) \rightarrow {}^2E_g$ and $^2E_g \rightarrow {}^2T_{2g}(^2E_g)$ in Ti^{3+} ions, which are located within oxygen octahedra distorted along the <111> trigonal axis. The crystal field strength is Dq = 2379 cm^{-1}. The less intense bands are attributed to electronic transitions $^2B_{2g} \rightarrow {}^2E_g$, $^2B_{2g} \rightarrow {}^2B_{1g}$, $^2B_{2g} \rightarrow {}^2A_{1g}$ in Ti^{3+} ions within tetragonally distorted oxygen octahedra.

The physical reasons for trigonal and tetragonal distortions of the oxygen octahedra in the $Na_{0.5}Bi_{0.5}TiO_3$ crystal lattice are discussed. The models of Ti^{3+}-based centers affecting optical absorption and photoluminescence are proposed. The observed effects of heat treatment can be used to control the radiation flux during optical excitation of $Na_{0.5}Bi_{0.5}TiO_3$ crystal.

Funding. The study was supported by the Ministry of Education and Science of Ukraine (Research Project #0122U001228) and partially by the Czech Science Foundation under Project # 23-05578S.

Conflict of interest. The authors declare no conflicts of interest.

References

1. Dresselhaus, M., Dresselhaus, G., Cronin, S. B., Gomes Souza Filho, A. (2018). Absorption of Light in Solids. In: *Solid State Properties. Graduate Texts in Physics. Springer, Berlin, Heidelberg*.
2. Zak, P. P., Lapina, V. A., Pavich, T. A., Trofimov, A. V., Trofimova, N. N., & Tsaplev, Y. B. (2017). Luminescent materials for modern light sources. *Russian Chemical Reviews*, *86*(9), 831.
3. Luminescent Materials. Fundamentals and Applications. Edited by Mikhail G. Brik, Alok M. Srivastava, (2023). p. 302. *Published by De Gruyter. Walter de Gruyter GmbH, Berlin/Boston*.
4. Nag Bhargavi, G., & Khare, A. (2015). Luminescence studies of perovskite structured titanates: a review. *Optics and Spectroscopy*, *118*, 902-917.
5. Milanez, J., de Figueiredo, A. T., de Lazaro, S., Longo, V. M., Erlo, R., Mastelaro, V. R., Franco, R. W. A., Varela, E. L., & Varela, J. A. (2009). The role of oxygen vacancy in the photoluminescence property at room temperature of the $CaTiO_3$. *Journal of Applied Physics*, *106*(4).
6. Smolenskii, G. A., Isupov, V. A., Agranovskaya, A. I., & Popov, S. N. (1961). Ferroelectrics with diffuse phase transitions. *Soviet Physics-solid state*, *2*(11), 2584-2594.
7. Shvartsman, V. V., & Lupascu, D. C. (2012). Lead-free relaxor ferroelectrics. *Journal of the American Ceramic Society*, *95*(1), 1-26.
8. Priya, S., Nahm S. (Eds.). (2012) Lead-Free Piezoelectrics, chapher Sodium Bismute Titanate-Based Ceramics, pp. 255-290 *Springer New York, New York, NY*.
9. Groeting, M., Hayn, S., & Albe, K. (2011). Chemical order and local structure of the lead-free relaxor ferroelectric $Na_{1/2}Bi_{1/2}TiO_3$. *Journal of Solid State Chemistry*, *184*(8), 2041-2046.
10. He, C., Zhang, Y., Sun, L., Wang, J., Wu, T., Xu, F., Du, Ch., Zhu, K. & Liu, Y. (2013). Electrical and optical properties of Nd^{3+}-doped $Na_{0.5}Bi_{0.5}TiO_3$ ferroelectric single crystal. *Journal of Physics D: Applied Physics*, *46*(24), 245104.
11. Jones, G. O., & Thomas, P. A. (2002). Investigation of the structure and phase transitions in the novel A-site substituted distorted perovskite compound $Na_{0.5}Bi_{0.5}TiO_3$. *Structural Science*, *58*(2), 168-178.
12. Dorcet, V., Trolliard, G., & Boullay, P. (2008). Reinvestigation of phase transitions in $Na_{0.5}Bi_{0.5}TiO_3$ by TEM. Part I: First order rhombohedral to orthorhombic phase transition. *Chemistry of Materials*, *20*(15), 5061-5073.
13. Trolliard, G., & Dorcet, V. (2008). Reinvestigation of phase transitions in $Na_{0.5}Bi_{0.5}TiO_3$ by TEM. Part II: Second order orthorhombic to tetragonal phase transition. *Chemistry of materials*, *20*(15), 5074-5082.
14. Gomah-Pettry, J. R., Saïd, S., Marchet, P., & Mercurio, J. P. (2004). Sodium-bismuth titanate based lead-free ferroelectric materials. *Journal of the European Ceramic Society*, *24*(6), 1165-1169.
15. Levanyuk, A. P., Sigov, A. S. (1988) Defects and structural phase transitions. *N.Y., London, Paris: Gordon& Breach Science Publishers.*
16. Sidak, V. M., & Trubitsyn, M. P. (2021). Dielectric relaxation and the dipole defects in Na0.5Bi0.5TiO3 single crystal. *Applied Nanoscience*, 775-780.
17. Kruzina, T. V., Sidak, V. M., Trubitsyn, M. P., Popov, S. A., & Suchanicz, J. (2014). Thermal treatment and dielectric properties of $Na_{0.5}Bi_{0.5}TiO_3$ single crystal. *Ferroelectrics*, *462*(1), 140-144.
18. Kruzina, T., Sidak, V., Trubitsyn, M., Popov, S., Tuluk, A., & Suchanicz, J. (2018). Impedance Spectra of As-Grown and Heat Treated $Na_{0.5}Bi_{0.5}TiO_3$ Crystals. *Acta Physica Polonica A*, *133*(4), 816-818.
19. He, C., Yi, X., Wu, T., Wang, J., Zhu, K., & Liu, Y. (2014). Wavelength dependence of refractive index in lead-free $Na_{0.5}Bi_{0.5}TiO_3$–$BaTiO_3$ single crystals. *Optical Materials*, *36*(12), 2023-2025.
20. Takenaka, T., & Nagata, H. (2012). Sodium bismuth titanate-based ceramics. *Lead-free piezoelectrics*, 255-290.
21. Scharfschwerdt, R., Mazur, A., Schirmer, O. F., Hesse, H., & Mendricks, S. (1996). Oxygen vacancies in $BaTiO_3$. *Physical Review B*, *54*(21), 15284.
22. Lenjer, S., Schirmer, O. F., Hesse, H., & Kool, T. W. (2002). Conduction states in oxide perovskites: Three manifestations of Ti^{3+} Jahn-Teller polarons in barium titanate. *Physical Review B*, *66*(16), 165106.
23. Henderson, B., & Imbusch, G. F. (2006). *Optical spectroscopy of inorganic solids* (Vol. 44). Oxford University Press.
24. Laguta, V. V., Glinchuk, M. D., Kuzian, R. O., Nokhrin, S. N., Bykov, I. P., Rosa, J., Jastrab´ık, L., & Karkut, M. G. (2002). The photoinduced Ti^{3+} centre in $SrTiO_3$. *Journal of Physics: Condensed Matter*, *14*(50), 13813.
25. Bersuker, I. B. (1986), Electronic structure and properties of coordination compounds: Introduction to the theory. *Khimiya, Leningrad*, 288 p.
26. Tyunina, M., Peräntie, J., Kocourek, T., Saukko, S., Jantunen, H., Jelinek, M., & Dejneka, A. (2020). Oxygen vacancy dipoles in strained epitaxial $BaTiO_3$ films. *Physical Review Research*, *2*(2), 023056.
27. Schmetzer, K., Bank, H. (1980) Explanation of absorption spectra of natural and synthetic Fe- and Ti-containing corundums. *Neues Jahrbuch für Mineralogie – Abhandlungen,* 130 (2), 216-225.

28. Jagło, G., Kluczewska-Chmielarz, K., Suchanicz, J., Kruk, A., Kania, A., Sitko, D., Nowakowska-Malczyk, M., Łapiński, M., & Stachowski, G. (2025). New insights into structural, optical, electrical and thermoelectric behavior of $Na_{0.5}Bi_{0.5}TiO_3$ single crystals. *Scientific Reports*, *15*(1), 2733.
29. Sidak, V. M., Trubitsyn, M. P., Panchenko, T. V. (2022) Dielectric relaxation induced by oxygen vacancies in $Na_{0.5}Bi_{0.5}TiO_3$ ceramics. *Condensed Matter Physics*. 25(4), 43705:1-10.
30. Sidak, V. M., & Trubitsyn, M. P. (2022, August). Dielectric Anomaly and Space Charge Polarization in Single Crystals of $Na_{0.5}Bi_{0.5}TiO_3$ and $Na_{0.5}Bi_{0.5}TiO_3$–$BaTiO_3$. In *International Conference on Nanotechnology and Nanomaterials* (pp. 365-382). Cham: Springer Nature Switzerland.
31. Back, M., Ueda, J., Xu, J., Asami, K., Amidani, L., Trave, E., & Tanabe, S. (2019). Uncovering the origin of the emitting states in Bi^{3+}-activated $CaMO_3$ (M= Zr, Sn, Ti) perovskites: Metal-to-metal charge transfer versus s–p transitions. *The Journal of Physical Chemistry C*, *123*(23), 14677-14688.
32. Srivastava, A. M. (2016). Luminescence of Bi3+ in the orthorhombic perovskites $CaB^{4+}O_3$ (B^{4+}= Zr, Sn): crossover from localized to D-state emission. *Optical Materials*, *58*, 89-92.
33. Van Steensel, L. I., Bokhove, S. G., Van de Craats, A. M., De Blank, J., & Blasse, G. (1995). The luminescence of Bi^{3+} in $LaInO_3$ and some other perovskites. *Materials Research Bulletin*, *30*(11), 1359-1362.

T. V. Panchenko, V. M. Sidak, M. P. Trubitsyn, V. Laguta, O. V. Khmelenko, T. V. Kruzina. (2025). Heat Treatment Effect on Optical Absorption and Photoluminescence in $Na_{0.5}Bi_{0.5}TiO_3$ Crystals**.** *Ukrainian Journal of Physical Optics*, *26*(4), 4001 – 04012.
doi: 10.3116/16091833/Ukr.J.Phys.Opt.2025.04001

Анотація. *Досліджено спектри оптичного поглинання та фотолюмінесценції у вирощених і термічно оброблених монокристалах натрій-вісмутового титанату* $Na_{0,5}Bi_{0,5}TiO_3$*. Термічний відпал проводився у повітрі та у вакуумі при температурі відпалу Tann = 1070 К. Оптичне поглинання та фотолюмінесценцію вимірювали в спектральному діапазоні 1,5–3,3 еВ. Встановлено, що відпал у повітрі зменшує оптичне поглинання, тоді як подальший відпал у вакуумі – збільшує його. Збудження термічно необробленого вирощеного кристалу поблизу межі фундаментального оптичного поглинання (~2,95 еВ) викликає інтенсивну фіолетову (~2,83 еВ) та слабку зелену (~2,25 еВ) фотолюмінесценцію. Відпал як у повітрі, так і у вакуумі зменшує інтенсивність як фіолетової, так і зеленої фотолюмінесценції. Вплив відпалу на оптичне поглинання та фотолюмінесценцію пов'язаний з електронними переходами у центрах* Ti^{3+}*, які компенсують надлишковий заряд кисневих вакансій і розташовані в тригонально та тетрагонально спотворених кисневих октаедрах.*

Ключові слова*: оптичне поглинання, фотолюмінесценція, відпал, вакансії кисню, кристал* $Na_{0,5}Bi_{0,5}TiO_3$